Aggregate and single-crystalline elasticity of hcp cobalt at high pressure

D. Antonangeli,[1,2] M. Krisch,[1] G. Fiquet,[3] J. Badro,[3,2] D. L. Farber,[2] A. Bossak,[1] and S. Merkel[4,*]
[1]*European Synchrotron Radiation Facility, Boîte Postale 220, F-38043 Grenoble Cedex, France*
[2]*Earth Science Division, Energy and Environment Directorate, Lawrence Livermore National Laboratory, 7000 East Avenue, Livermore, California 94550, USA*
[3]*Institut de Minéralogie et de Physique des Milieux Condensés, UMR CNRS 7590, Institut de Physique du Globe de Paris, Université Paris 6, 4 Place Jussieu, 75252 Paris Cedex 05, France*
[4]*Institute for Solid State Physics, University of Tokyo, Kashiwa, Chiba, Japan*
(Received 1 June 2005; revised manuscript received 4 August 2005; published 14 October 2005)

The longitudinal acoustic phonon dispersion of polycrystalline cobalt was determined by inelastic x-ray scattering up to 99 GPa, throughout the entire stability field of the hcp phase. The obtained aggregate compressional and shear sound velocities are compared with recent single crystal results, impulsive stimulated light scattering and ambient pressure ultrasonic measurements, as well as first principle calculations. We observe a linear evolution of the sound velocities with density up to 75 GPa. In this pressure range, the aggregate elastic properties of the polycrystalline sample are reproduced within 3% by a Voigt-Reuss-Hill average of the single crystal C_{ij}. Above 75 GPa both aggregate velocities show a softening. Our comparative analysis of single-crystalline and polycrystalline results points towards a magnetic origin of the anomaly.

DOI: 10.1103/PhysRevB.72.134303 PACS number(s): 63.20.−e, 62.50.+p, 62.20.Dc, 61.10.Eq

I. INTRODUCTION

The high-pressure properties of hexagonal-closed-packed (hcp) metals have recently attracted a lot of interest. These elements are indeed important model systems to test first principle calculations[1] and present intriguing properties such as, for example, the eventual existence of an electronic topological transition in zinc[2] and osmium,[3] or the interplay between magnetism and structure in the case of the bcc-to-hcp transition in iron.[4] A further important case is related to the elasticity of hcp iron, the main constituent of the Earth's core.[5,6] While nowadays the elastic anisotropy of the Earth's inner core is well established,[7,8] the origin of this anisotropy is still poorly understood, and the elasticity of hcp iron is still debated.[1,9–11]

Cobalt is a 3*d* transition metal with mechanical and thermal properties close to iron. Most importantly, athermal *ab initio* calculations[1] show that hcp Fe and hcp Co display a very similar pressure evolution of the elastic moduli and an analog elastic anisotropy. These theoretical results were recently validated by the direct measurements of the single-crystal elastic moduli of cobalt up to 39 GPa.[12] Moreover, Co presents a not-understood anomalous elastic behavior approaching the hcp-to-fcc structural transition,[13] possibly linked with high-pressure effects on the magnetic moment.[1,14] Magnetoelastic effects can than be investigated, complementing and extending the results obtained on single crystal[12] with results on polycrystalline sample, which can be more easily obtained at higher pressures, up to the structural transition.

At ambient conditions, cobalt is known to be ferromagnetic, existing in either the stable hcp phase or the metastable fcc phase. At high temperature, Co undergoes a phase transition around 695 K from the hcp to the fcc structure, and subsequently, via an isostructural transition, to a paramagnetic phase with a Curie temperature of 1400 K.[15] The temperature driven hcp-fcc transition exhibits no significant softening of most of the phonon branches, but only a decrease of about 27% in the C_{44} hexagonal shear constant[16] linked to the shear strain associated with the displacive martensitic transition.[17] Furthermore, no change in the magnetic moment occurs during the structural transition.[15,18]

At ambient temperature the hcp phase is stable up to 100 GPa, and then transforms martensitically to the fcc phase in the 105–150 GPa pressure range.[19] Density and compressibility considerations on one hand,[19] and first-principle calculations[15,19] on the other, suggest a nonmagnetic fcc phase, but there is to date no direct experimental evidence. Recent impulsive stimulated light scattering (ISLS) and Raman measurements[13] observed an anomalous density dependence of the aggregate elastic constants and of the E_{2g} mode Grüneisen parameter, at about 60 GPa, well below the phase transition. Magnetoelastic coupling and a collapse of the magnetic moment were suggested as possible causes for this behavior and *ab initio* calculations[1,14] support this scenario. However, further experimental work is needed to confirm these observations and, above all, to address the possible mechanisms responsible for the high-pressure elastic anomalies.

Here we present the experimental determination of the longitudinal acoustic phonon dispersion in polycrystalline cobalt up to 99 GPa obtained using inelastic x-ray scattering (IXS). We derived the aggregate compressional and shear sound velocities and analyzed our data in comparison with properly averaged single-crystal results, previously obtained by IXS.[12] This type of comparative study of aggregate and single-crystalline elasticity is essential in providing quantitative estimates for the various proposed mechanisms of the observed elastic anomaly, including texturing effects of polycrystalline hcp cobalt.

The paper is organized as follows: in Sec. II the IXS experiment is briefly described, while Sec. III is devoted to the presentation and discussion of the results. The polycrystalline results are compared to the single crystal averages and

the possible causes responsible for the high-pressure elastic anomalies are considered. Our main conclusions are summarized in Sec. IV.

II. EXPERIMENTAL DETAILS

We performed measurements on the IXS beamline II (ID28) at the European Synchrotron Radiation Facility in Grenoble, France. The instrument was operated in the Si(8,8,8) configuration, with an incident photon energy of 15.817 keV and a total instrumental energy resolution of 5.5 meV full width at half maximum (FWHM). The transverse dimensions of the focused x-ray beam of $25 \times 60\ \mu m^2$ (horizontal $\times$ vertical, FWHM) were further reduced by slits at the highest pressures. The momentum transfer $Q=2k_i \sin(\theta_s/2)$, where k_i is the incident photon wave vector and θ_s is the scattering angle, was selected by rotating the spectrometer around a vertical axis passing through the scattering sample in the horizontal plane. The momentum resolution was set by slits in front of the analyzers to 0.25 nm^{-1}. Energy scans were performed by varying the monochromator temperature while the analyzer temperature was kept fixed. Conversion from the temperature scale to the energy scale was accomplished by the following relation: $\Delta E/E=\alpha \times \Delta T$, where $\alpha=2.58\times10^{-6}\ K^{-1}$ is the linear thermal expansion coefficient of silicon at room temperature.[20] The validity of this conversion was checked by comparing the experimentally determined energies of the longitudinal acoustic and optical phonons of diamond with well-established inelastic neutron and Raman scattering results.[21,22] Further experimental details can be found elsewhere.[23]

99.99% purity cobalt powder was loaded in a rhenium gasket and pressurized in a diamond anvil cell without pressure transmitting medium. The investigated pressure range (0–99 GPa) was covered in three runs, using different cells. The scattering geometry was the standard one, with the x-ray beam along the main compression axis of the cell through the diamonds, and the momentum transfer approximatively perpendicular to it.

III. RESULTS AND DISCUSSION

A. IXS spectra and phonon dispersions

Representative examples of the collected IXS spectra are reported in Fig. 1. The spectra are characterized by an elastic contribution, centered at zero energy, and inelastic contributions from cobalt and diamond. Because of their higher sound velocity, the transverse acoustic (TA) and longitudinal acoustic (LA) phonons of diamond are located at higher energies with respect to cobalt. The longitudinal acoustic phonon of cobalt is therefore unambiguously identified as the peak between the elastic line and the diamond phonons. In order to have a robust determination of the zero energy position, in each scan the full elastic line has been recorded. The energy position $E(Q)$ of the phonons were extracted by fitting a set of Lorentzian functions convolved with the experimental resolution function to the IXS spectra, utilizing a standard χ^2 minimization routine.

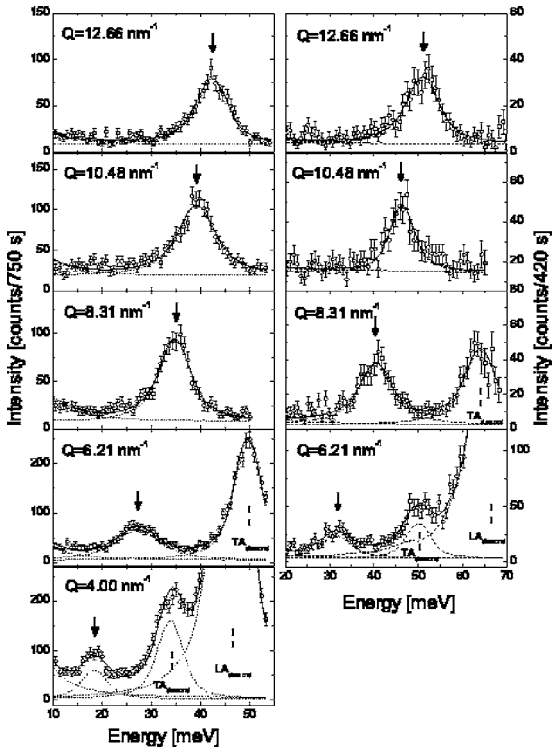

FIG. 1. Representative IXS spectra of polycrystalline hcp cobalt at 40 GPa (left panel) and 89 GPa (right panel) at the indicated momentum transfers Q. The experimental data are shown together with the best fit results (thick solid line) and the corresponding individual components (thin dotted line). For clarity only the inelastic peaks are shown. The arrows indicate the LA phonon of hcp Co, while the dashed marks point at the position of the LA and TA phonon of diamond, which are visible in the spectra at 4 and 6.21 nm^{-1} for $P=40$ GPa, and in the spectra at 6.21 nm^{-1} and 8.31 nm^{-1} for $P=89$ GPa. At 89 GPa the spectrum at 4 nm^{-1} is dominated by the very intense diamond phonons and the weak LA phonon of Co is not resolved.

Five to ten $E(Q)$ values were used to describe the LA phonon dispersions, which are reported, along with their best sine fit, in Fig. 2. For all pressures, the dispersion is very well described by a sine function, except for the highest pressure point (99 GPa), which is very close to the structural phase transition.

Within the framework of the Born–von Karman lattice-dynamics theory, and limiting us to the first term in the expansion (nearest neighbor interaction), the solution of the dynamical matrix can be written as[24]

$$E(\mathrm{meV}) = 4.192 \times 10^{-4} V_L(\mathrm{m/s}) Q_{max}(\mathrm{nm^{-1}}) \sin\left(\frac{\pi}{2}\frac{Q(\mathrm{nm^{-1}})}{Q_{max}(\mathrm{nm^{-1}})}\right), \quad (1)$$

where V_L is the compressional (longitudinal) sound velocity and Q_{max} is half the distance to the nearest reciprocal lattice point in the direction of Q. Values for V_L were consequently derived from the sine fit to the experimental dispersions, with Q_{max} left as a free parameter, while the shear (trans-

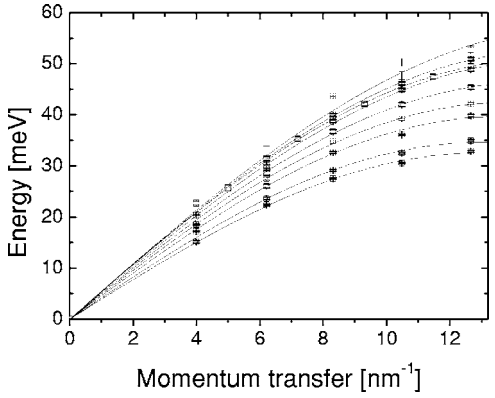

FIG. 2. *LA* phonon dispersion curves of polycrystalline hcp cobalt at ambient temperature and at pressures $P = 1.5, 11, 28, 40, 55, 70, 75, 89, 99$ GPa (from bottom to top). The displayed error bars of the energy position result from the experimental uncertainties, the statistical error of the fit, and the finite-Q resolution of the spectrometer. The lines through the data points are sine fits to the data.

verse) sound velocity V_T was obtained according to the relation

$$V_T^2 = \frac{3}{4}\left(V_L^2 - \frac{K}{\rho}\right), \tag{2}$$

where ρ is the density and K is the bulk modulus.

In parallel to the IXS spectra, the [100], [002], and [101] cobalt reflections were recorded. A strong reduction of the [002] reflection was observed with increasing pressure, leading to its complete disappearance above 55 GPa. This behavior is expected for the utilized diffraction geometry, because of the development of preferential alignment. Indeed, radial x-ray diffraction measurements have shown that the c axis of the crystallites has the tendency to align along the compression axis of the cell.[25] These diffraction measurements allowed us the direct determination of the density with an accuracy of better than 1%, and to cross-check both the values of Q_{max} as well as the pressure, determined by the ruby fluorescence and according to both the hydrostatic[19] and the nonhydrostatic hcp-Co equation of state.[25]

B. Aggregate sound velocities

The derived compressional sound velocity is plotted as a function of density in the upper panel of Fig. 3, together with results from ISLS (Ref. 13) and ultrasonic (US) measurements (Voigt-Reuss-Hill average[26] of single-crystal elastic moduli[27]), as well as from calculations.[1,14] The compressional sound velocity scales linearly with density, as expected within the quasi-harmonic approximation, up to 11.28 g/cm$^3 \leftrightarrow$ 75 GPa (solid line in Fig. 3). Above this value, approaching the martensitic hcp-to-fcc transition, a deviation from the linear behavior for $V_L(\rho)$ can be observed. This softening is also predicted in the same density region by the calculations, although theoretical values are systematically higher than the IXS ones. ISLS results show qualitatively the same trend as well, but the derived sound velocities are systematically lower than the IXS values, and lower than the ultrasonic results by ~5%, when back-extrapolated to ambient pressure.

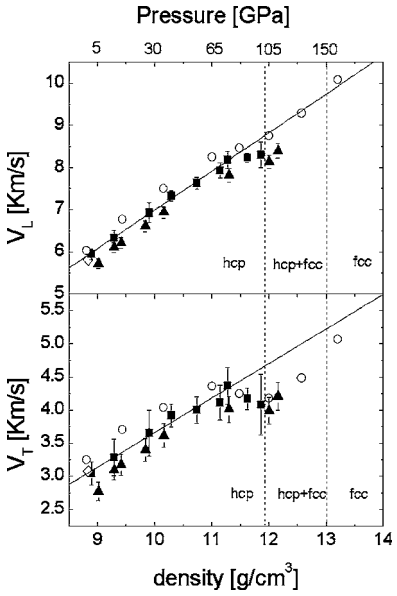

FIG. 3. Aggregate compressional (upper panel) and shear (lower panel) sound velocity of polycrystalline hcp cobalt as a function of density (the density errors are smaller than the symbols). The corresponding pressures are reported on the top axis. IXS results (full squares) and linear fit, taking into account data up to 11.28 g/cm^3 (75 GPa) (solid line); ambient pressure ultrasonic results (see Ref. 27; open diamond); *ab initio* calculations (see Ref. 14; open circles); ISLS measurements (see Ref. 13; solid triangles). The limits of the phase stability (Ref. 19) are indicated by dashed lines.

The IXS measurements of V_L have been combined with the nonhydrostatic hcp-cobalt equation of state,[25] in order to derive the density evolution of the shear velocity (the same values are also obtained using the hydrostatic equation of state[19]). The obtained V_T values are reported in the lower panel of Fig. 3 together with the results from calculations,[1,14] from ISLS (Ref. 13) and from US measurements (Voigt-Reuss-Hill average[26] of single-crystal results[27]). Due simply to the error propagation, the uncertainties in the IXS V_T are larger than for V_L. The linear evolution is, however, clearly visible up to 11.28 g/cm$^3 \leftrightarrow$ 75 GPa, as well as the softening (even more pronounced than for V_L) above this value. Once again the IXS results compare well with ambient pressure ultrasonic data and lie in-between the calculations and the ISLS measurements, which are respectively slightly too high and too low. The ISLS extrapolation for V_T to ambient pressure is well below the US results (~13%).

The V_L and V_T values, obtained by the different experimental techniques and the calculations, are summarized in Table I.

These observations indicate a regular evolution of the sound velocities up to a pressure point (P_{max}), above which, both the compressional and the shear aggregate sound velocities exhibit a softening. The departure from the linear behavior was suggested by Goncharov *et al.*[13] to start at lower pressure ($P_{max} \sim 60$ GPa $\leftrightarrow \sim 10.88$ g/cm^3), in contrast to the present IXS measurements, which clearly place P_{max} above 75 GPa.

TABLE I. Aggregate compressional and shear sound velocities for different pressures (densities) measured by IXS, ultrasounds (Ref. 27), ISLS (Ref. 13), and obtained from first principle calculations (Ref. 14). For IXS experiments the density is directly measured and cross-checked with the values determined from the cobalt hydrostatic (Ref. 19) and nonhydrostatic equation of state (Ref. 25). For the ISLS experiments the density is derived from the measured pressure according to the cobalt hydrostatic (Ref. 19) and nonhydrostatic equation of state (Ref. 25).

		IXS		US		ISLS		Calculations	
P (GPa)	ρ (g/cm^3)	V_L (m/s)	V_T (m/s)	V_L (m/s)	V_T (m/s)	V_L (m/s)	V_T (m/s)	V_L (m/s)	V_T (m/s)
	8.807							6030	3250
0	8.836			5810	3080				
1.5	8.899	5950±120	3040±120						
4.3	9.018					5720±110	2770±140		
11	9.292	6330±190	3280±180			6100±120	3100±150		
14.3	9.417					6220±120	3170±160		
	9.435							6780	3710
26	9.838					6600±130	3400±170		
28	9.908	6930±240	3650±340						
	10.160							7500	4030
36	10.165					6930±140	3620±180		
40	10.294	7330±120	3920±170						
55	10.740	7630±140	4000±200						
	11.006							8250	4360
70	11.150	7930±180	4110±260						
75	11.279	8180±200	4370±280						
76	11.305					7810±160	4010±200		
	11.484							8460	4250
89	11.627	8230±110	4170±160						
99	11.867	8300±300	4080±460						
105	12.005					8130±160	3990±200	8750	4180
112	12.162					8390±170	4210±210		
	12.576							9290	4490
	13.204							10080	5070

C. Comparison with single crystal results

Aggregate elastic properties, such as the bulk modulus K and the shear modulus G can be derived from the single-crystal elastic tensor, when an appropriate averaging scheme is employed. The Voigt average[28] is based on the assumption of a uniform strain field, and for hexagonal symmetry gives

$$K_V = \frac{1}{9}(2C_{11} + C_{33}) + \frac{2}{9}(2C_{13} + C_{12}), \tag{3}$$

$$G_V = \frac{1}{15}(2C_{11} + C_{33}) - \frac{1}{15}(2C_{13} + C_{12}) + \frac{1}{5}(2C_{44} + C_{66}). \tag{4}$$

The Reuss average[29] is based instead on the assumption of a uniform stress field, and for hexagonal symmetry gives

$$K_R = \frac{C_{33}(C_{11} + C_{12}) - 2C_{13}^2}{C_{11} + C_{12} + 2C_{33} - 4C_{13}}, \tag{5}$$

$$G_R = \frac{15}{4A(C_{11} + C_{12}) + 8AC_{13} + \frac{6}{C_{44}} + \frac{6}{C_{66}} + 2AC_{33}}, \tag{6}$$

with

$$\frac{1}{A} = C_{33}(C_{11} + C_{12}) - 2C_{13}^2. \tag{7}$$

Both averaging procedures ignore grain interactions, and are therefore quite crude approximations. They provide, however, rigorous bounds for the aggregate properties of a randomly oriented, macroscopically isotropic aggregate of crystals: it can be shown that the Voigt average is the lowest upper bound, while the Reuss average is the highest lower bound.[26] For isotropic crystals the two coincide. An empirical estimation currently used is the arithmetic mean of the two, the so-called Voigt-Reuss-Hill average. The aggregate velocities can then be calculated from K, G, and the density ρ according to

$$V_L^2 = \frac{1}{\rho}\left(K + \frac{4}{3}G\right) \tag{8}$$

$$V_T^2 = \frac{G}{\rho}. \tag{9}$$

In order to compare the IXS results obtained on powders with the ones obtained on single crystal,[12] the latter need to be extrapolated up to 99 GPa. Five independent acoustic phonon branches were used to determine the single-crystal elastic moduli C_{ij} to 39 GPa.[12] For the extrapolation we used two different approaches. In the first case we linearly extrapolated the velocity vs density data for each mode[31] and then solved the Christoffel equations[30] to derive the elastic moduli. Alternatively, the estimated[12] linear pressure evolutions of the C_{ij} is used. The results obtained by these two procedures differ by about 3% at 99 GPa and even less at lower pressures, except for C_{13}, where the difference starts to be significant already at 50 GPa, and is about 20% at 99 GPa. However, the two extrapolations yield results for the aggregate bulk and shear moduli within 1% below 50 GPa and within 2% at 99 GPa. In the following, we will consider the arithmetic average of the values obtained by these two procedures for the various C_{ij}.

The bulk modulus, the shear modulus and the aggregate compressional and shear sound velocities were computed according to the Voigt, Reuss, and Voigt-Reuss-Hill average. Voigt and Reuss determinations differ by only 1% at 99 GPa and even less at lower pressures. Thus, the single-crystal anisotropy is only very weakly reflected in the effective elastic anisotropy of the aggregate, when a completely random distribution of crystallites is considered.

The density evolution of the aggregate compressional[32] sound velocity is illustrated in Fig. 4, where the IXS results obtained on powders are reported together with the ambient pressure ultrasonic determination[27] and the Voigt-Reuss-Hill average of the single-crystal elastic moduli.[12] Despite a different slope, the two IXS data sets up to 75 GPa differ by less than 3%, thus testifying that a simple, randomly oriented distribution describes quite well the elastic properties of the polycrystal under compression. Moreover, according to this observation, a regular behavior of the various C_{ij} with increasing pressure is expected above the directly investigated pressure range (0–39 GPa),[12] likely up to 75 GPa.

Above 75 GPa the discrepancy between the polycrystalline and the single-crystal averaged results starts to be significant. The observed deviation from linearity in $V_L(\rho)$ and $V_T(\rho)$ could be considered as a precursor effect of the martensitic hcp-to-fcc structural transition, which manifests itself by an important softening of one or more elastic moduli. Such transition in cobalt can be induced both by pressure and temperature.[19] For the temperature-induced hcp-to-fcc transition, a softening of C_{44} by about 27% in the close vicinity of the transition was observed, while the other elastic moduli remained unaffected.[16] If the same amount of softening of C_{44} is applied to the present pressure-induced case, for the two highest pressure points (89 and 99 GPa), we can recompute the averaged V_L, and the resulting values are lower by about 1.5%, whereas the IXS experiments on the polycrystalline sample display a difference from the linear extrapolation by about 3% and 4.5% (89 GPa and 99 GPa, respectively). Moreover, in the present case, the nonlinear density dependence was observed well before the transition. These considerations, together with the proposed simple estimation, suggest that the observed anomaly in V_L is not likely due to the shear strain associated with the hcp-to-fcc transition, as in the temperature-driven case.[17]

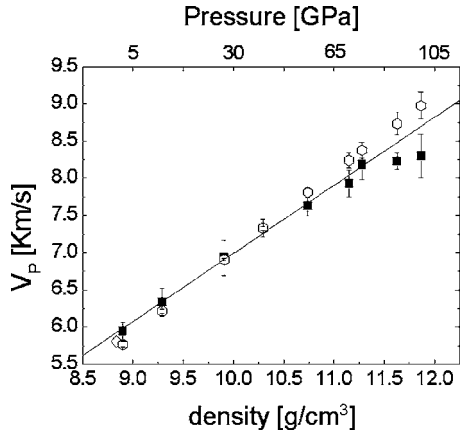

FIG. 4. Aggregate compressional sound velocity V_L of hcp cobalt as a function of density (the corresponding pressure values are indicated in the top axis). Errors on density are smaller than the symbols. Squares: IXS results obtained on powders; open diamonds: ambient pressure ultrasonic results (Ref. 27); open hexagons: Voigt-Reuss-Hill average of single crystal elastic moduli, obtained by IXS (Ref. 12) and extrapolated to 99 GPa. The solid line is an extrapolated linear fit to the powder data below 11.28 g/cm^3 (75 GPa).

Ab initio calculations[14] predict a departure from linearity in the same density region as the experimental IXS observations (see Fig. 3). The proposed mechanism is a reduction of the magnetic moment, concomitant with an evident softening of C_{44} and C_{66}. In order to compare these theoretical findings with the IXS results, the theoretical C_{ij} were scaled to the experimentally determined ones (IXS single-crystal results). The thus-obtained C_{ij} exhibit an important softening of C_{44}, a moderate hardening of C_{13}, and a slight softening of all the elastic moduli at pressure of about 85 GPa (ρ=11.48 g/cm^3,57.5 bohrs^3). The aggregate V_L, once recalculated using the Voigt-Reuss-Hill average, then shows a reduction of about 2.5%. The so-obtained anomaly in the elastic moduli thus reproduces quite well our experimentally determined trend (3% softening at 89 GPa).

The good agreement between the extrapolated single crystal aggregate averages and our polycrystalline measurements suggest that the effects of texture in our samples are minimal. However, as there exist experimental data on the textural evolution in polycrystalline Co, we quantitatively treat these effects below. Recent radial x-ray diffraction measurements (RXRD) on quasiuniaxially compressed polycrystalline cobalt reveal an alignment of the c axis of the crystallites along the compression axis of the cell, with a cylindrical

symmetry.[25] Most of this texture is developed within the first 5 GPa and up to the highest investigated pressure of 42 GPa, the increasing stress essentially modifies the degree of alignment, not the symmetry. At the highest investigated pressure the maximum pole density is 3.17 multiples of a random distribution. On the basis of these results we can recompute the properly weighted orientationally averaged V_L. The aggregate V_L values, corrected for these texture effects as well as the scattering geometry (momentum transfer perpendicular to the compression axis of the cell) differ from the Voigt-Reuss-Hill average (random distribution) by about 0.3% at 1.5 GPa and about 1% at 40 GPa, yielding slightly lower sound speeds.

According to the observation that most of the texture was already developed at 5 GPa, we can assume that the experimentally determined texture at 42 GPa is only very weakly dependent on pressure, and incorporate the effects of preferential orientation in the averaging process at 85 GPa, together with the theoretically estimated magnetoelastic effects. The resulting V_L exhibits a reduced softening of about 1.8%, as a consequence of the different weights of the various C_{ij}'s. According to this estimation, the texture developed by polycrystalline cobalt under nonhydrostatic compression, tends to reduce the aggregate elastic anomalies induced by the softening of the magnetic moment, and, since a further very strong evolution of the texture at high pressure is unlikely, cannot be considered the main cause responsible for the observed high-pressure anomalies in V_L and V_T.

IV. CONCLUSIONS

We have measured the aggregate longitudinal phonon dispersion of hcp cobalt up to 99 GPa, over the entire stability range of the hcp phase. The derived compressional and shear sound velocities exhibit a linear evolution with density up to 11.28 $g/cm^3 \leftrightarrow 75$ GPa. Above, a significant deviation from linearity is observed on approaching the hcp-to-fcc phase transition. Our IXS results were compared with the average velocities derived from the single-crystal elastic tensor,[12] with high-pressure ISLS (Ref. 13) and ambient pressure ultrasonic measurements,[27] and with *ab initio* calculations.[1,14] Our IXS data are in good agreement with the US results. This is in contrast to the ISLS data, especially for V_T, where the difference between the ISLS and US results is about 13%.

We suggest that the single-crystal elastic moduli vary linearly with pressure to 75 GPa. In this pressure range, the aggregate elastic properties of the polycrystalline sample are reproduced within 3% by a Voigt-Reuss-Hill average of the single crystal C_{ij},[12] indicating that a simple, macroscopically isotropic, randomly oriented distribution, already provides a quite good general description of cobalt powder. When the effects of texture are considered, V_L changes in the 0–40 GPa range, at the most by 1%, slightly improving the agreement between the IXS powder and the properly averaged single-crystal results.

Above 75 GPa the IXS measurements show a softening of the aggregate velocities, in agreement with calculations. The same trend is also reproduced by ISLS measurements, although the departure from linearity was proposed to start at lower pressure. The comparison of polycrystalline and single-crystal IXS results with theoretical calculations allows us to provide quantitative estimates for the various proposed mechanism of this elastic anomaly. A precursor effect of the martensitic hcp-to-fcc phase transition—as for the temperature-driven transition to the fcc phase—seems unlikely, since the corresponding reduction of C_{44} by 27% (Ref. 16) is not enough to explain the IXS results. Furthermore, this softening occurs only in a narrow temperature range, very close to the phase transition, while in the present high-pressure experiment, the softening is already observed well below the transition pressure. A magnetoelastic effect, associated with a reduction of the magnetic moment, as suggested by Goncharov *et al.*[13] and supported by calculations,[1,14] appears to be the driving mechanism. The deviation from linearity in $V_L(\rho)$ is indeed qualitatively reproduced by our estimate on the basis of the extrapolation of the experimental C_{ij}. The remaining quantitative discrepancy could be explained by thermal correction to the athermal calculations.

A scenario analogous to the one recently proposed for the bcc-to-hcp transition in iron,[4] characterized by a magnetic transition preceding the structural one, can be envisaged. Thus, the origin of the instability of the hcp Co with increasing pressure can be ascribed to the effect of pressure on the magnetic moment. A direct experimental determination of the pressure evolution of the magnetic moment is, however, highly recommended to confirm this hypothesis.

ACKNOWLEDGMENTS

D. Gambetti and D. Gibson are acknowledged for their technical assistance. The authors wish to thank M. Hanfland for the use of the high-pressure laboratory and for unscheduled diffraction measurements. We highly appreciated the discussions with F. Guyot.

*Present address: Department of Earth and Planetary Science, University of California, Berkeley, CA, 94720.

[1] G. Steinle-Neumann, L. Stixrude, and R. E. Cohen, Phys. Rev. B **60**, 791 (1999); **69**, 219903(E) (2004).

[2] S. Klotz, M. Braden, and J. M. Besson, Phys. Rev. Lett. **81**, 1239 (1998).

[3] F. Occelli, D. L. Farber, J. Badro, C. M. Aracne, D. M. Teter, M. Hanfland, B. Canny, and B. Couzinet, Phys. Rev. Lett. **93**, 109901(E) (2004).

[4] O. Mathon, F. Baudelet, J. P. Itié, A. Polian, M. d'Astuto, J. C. Chervin, and S. Pascarelli, Phys. Rev. Lett. **93**, 255503 (2004).

[5] F. Birch, J. Geophys. Res. **57**, 227 (1952).

[6] A. Jephcoat and P. Olson, Nature **325**, 332 (1987).
[7] J. H. Woodhouse, D. Giardini, and X. D. Li, Geophys. Res. Lett. **13**, 1549 (1986).
[8] K. G. Creager, Nature **356**, 309 (1992).
[9] L. Stixrude and R. E. Cohen, Science **267**, 1972 (1995).
[10] H. K. Mao, J. Shu, G. Shen, R. J. Hemley, B. Li, and A. K. Singh, Nature **396**, 741 (1998); correction, **399**, 280 (1999).
[11] D. Antonangeli, F. Occelli, H. Requardt, J. Badro, G. Fiquet, and M. Krisch, Earth Planet. Sci. Lett. **225**, 243 (2004).
[12] D. Antonangeli, M. Krisch, G. Fiquet, D. L. Farber, C. M. Aracne, J. Badro, F. Occelli, and H. Requardt, Phys. Rev. Lett. **93**, 215505 (2004).
[13] A. F. Goncharov, J. Crowhurst, and J. M. Zaug, Phys. Rev. Lett. **92**, 115502 (2004).
[14] G. Steinle-Neumann (private communication).
[15] C. S. Yoo, P. Söderlind, and H. Cynn, J. Phys.: Condens. Matter **10**, L311 (1998).
[16] B. Strauss, F. Frey, W. Petry, J. Trampenau, K. Nicolaus, S. M. Shapiro, and J. Bossy, Phys. Rev. B **54**, 6035 (1996).
[17] P. Toledano, G. Krexner, M. Prem, H.-P. Weber, and V. P. Dmitriev, Phys. Rev. B **64**, 144104 (2001).
[18] P. Lazor, Ph.D. thesis, Uppsala University, 1994.
[19] C. S. Yoo, H. Cynn, P. Söderlind, and V. Iota, Phys. Rev. Lett. **84**, 4132 (2000).
[20] A. Bergamin, G. Cavagnero, and G. Mana, J. Appl. Phys. **82**, 5396 (1997).
[21] J. Kulda, H. Kainzmaier, D. Strauch, B. Dorner, M. Lorenzen, and M. Krisch, Phys. Rev. B **66**, 241202(R) (2002).
[22] R. Verbeni (private communication).
[23] M. Krisch, J. Raman Spectrosc. **34**, 628 (2003).
[24] N. W. Ashcroft and N. D. Mermin, *Solid State Physics* (Saunders College Publishing, USA, 1976).
[25] S. Merkel, N. Miyajima, and T. Yagi (unpublished).
[26] R. Hill, Proc. Phys. Soc., London, Sect. A **65**, 349 (1952).
[27] H. R. Schober and H. Dederichs, *Elastic, Piezoelectric, Pyroelectric, Piezooptic, Electrooptic Constants and Nonlinear Dielectric Susceptibilities of Crystals*, edited by Landolt-Börnstedt, New Series III, (Springer, Berlin, 1979), Vol. 11a.
[28] W. Voigt, *Lehrbuch der Kristallphysik* (Teubner, Leipzig, 1928).
[29] A. Reuss, Z. Angew. Math. Mech. **9**, 55 (1929).
[30] B. A. Auld, *Acoustic Fields and Waves in Solids* (John Wiley & Sons, New York, 1973), Vol. 1.
[31] We recall that within the frame of the quasiharmonic approximation, sound velocities are supposed to scale linearly with density.
[32] In the following, only V_L will be considered, since it is directly determined, with a higher precision than V_T.